Inorganic Chemistry
Article

Self-Assembly and Host−Guest Interaction of Metallomacrocycles Using Fluorescent Dipyrazole Linker with Dimetallic Clips

Guo-Hong Ning,[†] Liao-Yuan Yao,[†] Li-Xia Liu,[†,‖] Ting-Zheng Xie,[†] Yi-Zhi Li,[‡] Yu Qin,[*,‡] Yuan-Jiang Pan,[§] and Shu-Yan Yu[*,†]

[†]*Laboratory for Self-Assembly Chemistry, Department of Chemistry, Renmin University of China, Beijing 100872, China,* [‡]*Department of Chemistry, State Key Laboratory of Coordination Chemistry, Coordination Chemistry Institute and Key Lab of Analytical Chemistry for Life Science, Ministry of Education, Nanjing University, Nanjing 210093, People's Republic of China, and* [§]*Department of Chemistry, Zhejiang University, Hangzhou 310027, People's Republic of China.* [‖]*Present address: Department of Chemistry and Biochemistry, Auburn University, Auburn, Alabama 36849.*

By employing diimine ligands coordinated dimetallic clips ([(bpy)$_2$Pd$_2$(NO$_3$)$_2$](NO$_3$)$_2$ or [(phen)$_2$Pd$_2$(NO$_3$)$_2$](NO$_3$)$_2$, where bpy = 2,2′-bipyridine, phen = 1,10-phenanthroline) as the corner and anthracene-, naphthalene-, and benzene-based dipyrazolate dianions as the linker, a series of positively charged metallomacrocycles ([M$_4$L$_2$]$^{4+}$ or [M$_8$L$_4$]$^{8+}$) have been synthesized through a directed self-assembly method in aqueous solution. Every macrocycle has a cavity to bind solvent molecules or anions. The structures were characterized by elemental analysis, ^{1}H and ^{13}C NMR, electrospray ionization mass spectrometry, and single crystal X-ray diffraction analysis for compound **1**·4PF$_6$$^-$ (**1** = {[(bpy)Pd]$_4$L^1$_2$}$^{4+}$), **3**·4PF$_6$$^-$·8CH$_3$CN·H$_2$O (**3** = {[(bpy)Pd]$_4L^2_2$}$^{4+}$), and **7**·4PF$_6$$^-$·6H$_2$O (**7** = {[(bpy)Pd]$_4L^5_2$}$^{4+}$). The 1:1 host−guest complexation for anthracene-based dipyrazolate-bridged macrocycles with aromatic guests was investigated via UV−vis and fluorescent titration.

Introduction

In the past two decades, significant progress has made in the development of supramolecular self-assembly.[1,2] A large number of macrocyclic or cage-like structures have been obtained by rationally designed metal directional self-assembly approach,[1−3] which has attracted a great deal of attention in recent years not only because of their structure diversity such as molecular triangles,[3,4,6−8] squares and rectangles,[3,5−10] pentagons and hexagons,[11] bowls and cages,[12] cuboctahedra and dodecahedra,[13] helicates, grids, catenanes, nanotubes and polytubes,[14] and so on,[15] but also due to the rich physical properties of the metal-assembled systems in magnetism, luminescence,[2] electron transfer,[9,10,16] and the exciting applications
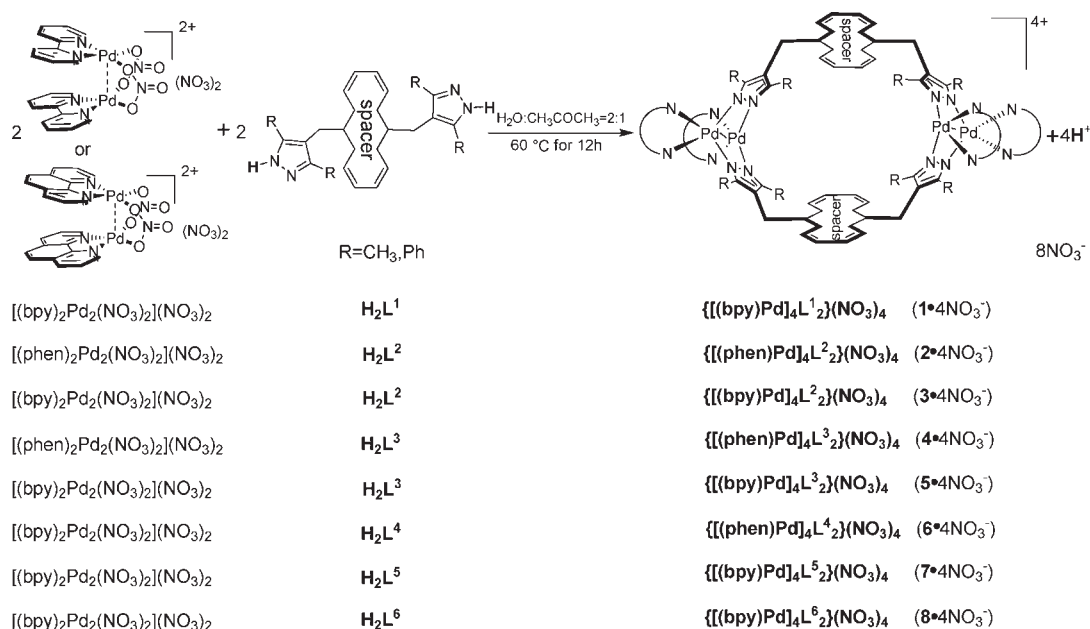
(1) Lehn, J.-M. *Supramolecular Chemistry, Concepts and Perspectives*; VCH: Weinheim, Germany, 1995.
(2) (a) *Science* **2002,** *295,* 2395-2421 (Supramolecular Chemistry and Self-Assembly, Special Issue). (b) Lindoy, L. F.; Atkinson, I. *Self-Assembly in Supramolecular Systems* (*Monographs in Supramolecular Chemistry*); Stoddart, J. F., Ed.; The Royal Society of Chemistry: London, 2000. (c) Fujita, M. *Molecular Self-Assembly Organic Versus Inorganic Approach* (*Structure and Bonding*); Springer: New York, 2000; Vol. 96. (d) Sauvage, J.-P. *Transition Metals in Supramolecular Chemistry, Perspectives in Supramolecular Chemistry*; Wiley: New York, 1999; Vol. 5. (e) Lehn, J.-M. Templating, Self-Assembly, and Self-Organization. In *Comprehensive Supramolecular Chemistry*; Sauvage, J.-P., Hosseini, M. W., Ed.; Pergamon: New York, 1996. (f) Desvergne, J. P.; Czarnik, A. W. *Chemosensors of Ion and Molecule Recognition*. Kluwe Academic Publisher: The Netherlands, 1996.

(3) (a) Fujita, M.; Tominaga, M.; Hori, A.; Therrien, B. *Acc. Chem. Res.* **2005,** *38,* 371–380. (b) Yu, S.-Y.; Li, S.-H.; Huang, H.-P.; Zhang, Z.-X.; Jiao, Q.; Shen, H.; Hu, X.-X.; Huang, H. *Curr. Org. Chem.* **2005,** *9,* 555–563. (c) Würthner, F.; You, C.-C.; Saha-Möller, C. R. *Chem. Soc. Rev.* **2004,** *33,* 133–146. (d) Seidel, S. R.; Stang, P. J. *Acc. Chem. Res.* **2002,** *35,* 972–983. (e) Cotton, F. A.; Lin, C.; Murillo, C. A. *Acc. Chem. Res.* **2001,** *34,* 759–771. (f) Dinolfo, P. H.; Hupp, J. T. *Chem. Mater.* **2001,** *13,* 3113–3125. (g) Leininger, S.; Olenyuk, B.; Stang, P. J. *Chem. Rev.* **2000,** *100,* 853–908. (h) Caulder, D. L.; Raymond, K. N. *Acc. Chem. Res.* **1999,** *32,* 975–982. (i) Navarro, J. A. R.; Lippert, B. *Coord. Chem. Rev.* **1999,** *185−186,* 653–667. (j) Fujita, M. *Acc. Chem. Res.* **1999,** *32,* 53–61. (k) Fujita, M. *Chem. Soc. Rev.* **1998,** *27,* 417–425. (l) Slone, R. V.; Benkstein, K. D.; Bélanger, S.; Hupp, J. T.; Guzei, I. A.; Rheingold, A. L. *Coord. Chem. Rev.* **1998,** *171,* 221–243. (m) Stang, P. J. *Chem. -Eur. J.* **1998,** *4,* 19–27. (n) Stang, P. J.; Olenyuk, B. *Acc. Chem. Res.* **1997,** *30,* 502–518. (o) Fujita, M.; Ogura, K. *Coord. Chem. Rev.* **1996,** *148,* 249–264.
(4) (a) Papaefstathiou, G. S.; Hamilton, T. D.; MacGillivray, L. R. *Chem. Commun.* **2004,** *3,* 270–271. (b) Schnebeck, R.-D.; Freisinger, E.; Glahe, F.; Lippert, B. *J. Am. Chem. Soc.* **2000,** *122,* 1381–1390. (c) Schnebeck, R.-D.; Freisinger, E.; Lippert, B. *Chem. Commun.* **1999,** *8,* 675–676. (d) Schnebeck, R.-D.; Randaccio, L.; Zangrando, E.; Lippert, B. *Angew. Chem., Int. Ed.* **1998,** *37,* 119–121.
(5) (a) Angaridis, P.; Berry, J. F.; Cotton, F. A.; Murillo, C. A.; Wang, X. *J. Am. Chem. Soc.* **2003,** *125,* 10327–10334. (b) Bera, J. K.; Angaridis, P.; Cotton, F. A.; Petrukhina, M. A.; Fanwick, P. E.; Walton, R. A. *J. Am. Chem. Soc.* **2001,** *123,* 1515–1516. (c) Cotton, F. A.; Daniels, L. M.; Lin, C.; Murillo, C. A.; Yu, S.-Y. *J. Chem. Soc., Dalton Trans.* **2001,** *121,* 502–504. (d) Cotton, F. A.; Daniels, L. M.; Lin, C.; Murillo, C. A. *J. Am. Chem. Soc.* **1999,** *121,* 4538–4539.

Scheme 1. Self-Assembly of $[M_4L_2]^{4+}$-Type Metallomacrocycles

[(bpy)₂Pd₂(NO₃)₂](NO₃)₂	H₂L¹	{[(bpy)Pd]₄L¹₂}(NO₃)₄ (1•4NO₃⁻)
[(phen)₂Pd₂(NO₃)₂](NO₃)₂	H₂L²	{[(phen)Pd]₄L²₂}(NO₃)₄ (2•4NO₃⁻)
[(bpy)₂Pd₂(NO₃)₂](NO₃)₂	H₂L²	{[(bpy)Pd]₄L²₂}(NO₃)₄ (3•4NO₃⁻)
[(phen)₂Pd₂(NO₃)₂](NO₃)₂	H₂L³	{[(phen)Pd]₄L³₂}(NO₃)₄ (4•4NO₃⁻)
[(bpy)₂Pd₂(NO₃)₂](NO₃)₂	H₂L³	{[(bpy)Pd]₄L³₂}(NO₃)₄ (5•4NO₃⁻)
[(bpy)₂Pd₂(NO₃)₂](NO₃)₂	H₂L⁴	{[(phen)Pd]₄L⁴₂}(NO₃)₄ (6•4NO₃⁻)
[(bpy)₂Pd₂(NO₃)₂](NO₃)₂	H₂L⁵	{[(bpy)Pd]₄L⁵₂}(NO₃)₄ (7•4NO₃⁻)
[(bpy)₂Pd₂(NO₃)₂](NO₃)₂	H₂L⁶	{[(bpy)Pd]₄L⁶₂}(NO₃)₄ (8•4NO₃⁻)

in selective guest inclusion, drug delivery, molecular recognition, catalysis, and biological mimicry.[1,3,6,12,13,17]

Chart 1

Aromatic guests

However, most of the self-assembled metallosupramolecular systems have been using single metal ions as the corner for coordinating with a variety of monodentate or chelating ligands. The isolated, structurally characterized metal−metal bonded or dimetal-interacted based finite molecular architectures play an

(6) (a) Fujita, M.; Sasaki, O.; Mitsuhashi, T.; Fujita, T.; Yazaki, J.; Yamaguchi, K.; Ogura, K. *Chem. Commun.* **1996**, *13*, 1535–1536. (b) Fujita, M.; Yazaki, J.; Ogura, K. *J. Am. Chem. Soc.* **1990**, *112*, 5645–5647.

(7) (a) Habereder, T.; Warchhold, M.; Nöth, H.; Severin, K. *Angew. Chem., Int. Ed.* **1999**, *38*, 3225–3228. (b) Lai, S.-W.; Chan, M. C.-W.; Peng, S.-M.; Che, C.-M. *Angew. Chem., Int. Ed.* **1999**, *38*, 669–671. (c) Thompson, A.; Rettig, S. J.; Dolphin, D. *Chem. Commun.* **1999**, *7*, 631–632. (d) Hall, J.; Loeb, S. J.; Shimizu, G. K. H.; Yap, G. P. A. *Angew. Chem., Int. Ed.* **1998**, *37*, 121–123. (e) Barbera, J.; Elduque, A.; Gimenez, R.; Oro, L. A.; Serrano, J. L. *Angew. Chem., Int. Ed.* **1996**, *35*, 2832–2835.

(8) (a) Graves, C. R.; Merlau, M. L.; Morris, G. A.; Sun, S.-S.; Nguyen, S. T.; Hupp, J. T. *Inorg. Chem.* **2004**, *43*, 2013–2017. (b) Ferrer, M.; Mounir, M.; Rossell, O.; Ruiz, E.; Maestro, M. A. *Inorg. Chem.* **2003**, *42*, 5890–5899. (c) Schweiger, M.; Seidel, S. R.; Arif, A. M.; Stang, P. J. *Inorg. Chem.* **2002**, *41*, 2556–2559. (d) Sautter, A.; Schmid, D. G.; Jung, G.; Würthner, F. *J. Am. Chem. Soc.* **2001**, *123*, 5424–5430. (e) Schnebeck, R.-D.; Freisinger, E.; Lippert, B. *Eur. J. Inorg. Chem.* **2000**, 1193–1200. (f) Sun, S.-S.; Lees, A. J. *J. Am. Chem. Soc.* **2000**, *122*, 8956–8967. (g) Sun, S.-S.; Lees, A. J. *Inorg. Chem.* **1999**, *38*, 4181–4182. (h) Lee, S. B.; Hwang, S.; Chung, D. S.; Yun, H.; Hong, J.-I. *Tetrahedron Lett.* **1998**, *39*, 873–876. (i) Mcquillan, F. S.; Berridge, T. E.; Chen, H.; Hamor, T. A.; Jones, C. J. *Inorg. Chem.* **1998**, *37*, 4959–4970. (j) Fujita, M.; Ogura, K. *Bull. Chem. Soc. Jpn.* **1996**, *69*, 1471–1482.
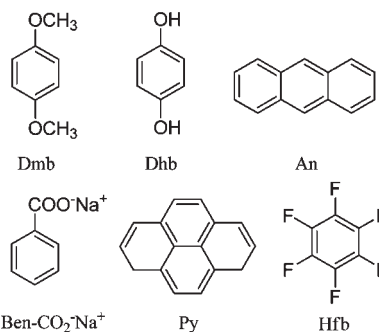
(9) (a) Würthner, F.; Sautter, A.; Schmid, D. G.; Weber, P. J. A. *Chem.−Eur. J.* **2001**, *7*, 894–902. (b) Sun, S.-S.; Silva, A. S.; Brinn, I. M.; Lees, A. J. *Inorg. Chem.* **2000**, *39*, 1344–1345. (c) Würthner, F.; Sautter, A. *Chem. Commun.* **2000**, *6*, 445–446. (d) Lahav, M.; Gabai, R.; Shipway, A. N.; Willner, I. *Chem. Commun.* **1999**, *19*, 1937–1938. (e) Campos-Fernandez, C. S.; Clerac, R.; Dunbar, K. R. *Angew. Chem., Int. Ed.* **1999**, *38*, 3477–3479. (f) Woessner, S. M.; Helms, J. B.; Houlis, J. F.; Sullivan, B. P. *Inorg. Chem.* **1999**, *38*, 4380–4381. (g) Slone, R. V.; Hupp, J. T.; Stern, C.; Albrecht-Schmitt, T. E. *Inorg. Chem.* **1996**, *35*, 4096–4097. (h) Slone, R. V.; Yoon, D. I.; Calhoun, R. M.; Hupp, J. T. *J. Am. Chem. Soc.* **1995**, *117*, 11813–11814. (i) Stang, P. J.; Cao, D. H.; Saito, S.; Arif, A. M. *J. Am. Chem. Soc.* **1995**, *117*, 6273–6283. (j) Stang, P. J.; Cao, D. H. *J. Am. Chem. Soc.* **1994**, *116*, 4981–4982.

(10) (a) Hartmann, H.; Berger, S.; Winter, R.; Fiedler, J.; Kaim, W. *Inorg. Chem.* **2000**, *39*, 4977–4980. (b) Benkstein, K. D.; Hupp, J. T.; Stern, C. L. *J. Am. Chem. Soc.* **1998**, *120*, 12982–12983. (c) Benkstein, K. D.; Hupp, J. T.; Stern, C. L. *Angew. Chem., Int. Ed.* **2000**, *39*, 2891–2893. (d) Woessner, S. M.; Helms, J. B.; Shen, Y.; Sullivan, B. P. *Inorg. Chem.* **1998**, *37*, 5406–5407. (e) Benkstein, K. D.; Hupp, J. T.; Stern, C. L. *Inorg. Chem.* **1998**, *37*, 5404–5405.

(11) (a) Matsumoto, N.; Motoda, Y.; Matsuo, T.; Nakashima, T.; Re, N.; Dahan, F.; Tuchagues, J.-P. *Inorg. Chem.* **1999**, *38*, 1165–1173. (b) Mamula, O.; von Zelewsky, A.; Bernardinelli, G. *Angew. Chem., Int. Ed.* **1998**, *37*, 289–293. (c) Stang, P. J.; Persky, N. E.; Manna, J. *J. Am. Chem. Soc.* **1997**, *119*, 4777–4778. (d) Hasenknopf, B.; Lehn, J.-M.; Baum, G.; Kneisel, B. O.; Fenske, D. *Angew. Chem., Int. Ed.* **1996**, *35*, 1838–1840.

(12) (a) Tashiro, S.; Tominaga, M.; Kawano, M.; Therrien, B.; Ozeki, T.; Fujita, M. *J. Am. Chem. Soc.* **2005**, *127*, 4546–4547. (b) Kusukawa, T.; Fujita, M. *J. Am. Chem. Soc.* **2002**, *124*, 13576–13582. (c) Yu, S.-Y.; Kusukawa, T.; Biradha, K.; Fujita, M. *J. Am. Chem. Soc.* **2000**, *122*, 2665–2666. (d) Fujita, M.; Fujita, N.; Ogura, K.; Yamaguchi, K. *Nature* **1999**, *400*, 52–55. (e) Fujita, M.; Yu, S.-Y.; Kusukawa, T.; Funaki, H.; Ogura, K.; Yamaguchi, K. *Angew. Chem., Int. Ed.* **1998**, *37*, 2082–2085.

(13) (a) Olenyuk, B.; Levin, M. D.; Whiteford, J. A.; Shield, J. E.; Stang, P. J. *J. Am. Chem. Soc.* **1999**, *121*, 10434–10435. (b) Olenyuk, B.; Whiteford, J. A.; Fechtenkötter, A.; Stang, P. J. *Nature* **1999**, *398*, 796–799.

(14) (a) Yamaguchi, T.; Tashiro, S.; Tominaga, M.; Kawano, M.; Ozeki, T.; Fujita, M. *J. Am. Chem. Soc.* **2004**, *126*, 10818–10819. (b) Biradha, K.; Aoyagi, M.; Fujita, M. *J. Am. Chem. Soc.* **2000**, *122*, 2397–2398. (c) Aoyagi, M.; Biradha, K.; Fujita, M. *J. Am. Chem. Soc.* **1999**, *121*, 7457–7458. (d) Takeda, N.; Umemoto, K.; Yamaguchi, K.; Fujita, M. *Nature* **1999**, *398*, 794–796.

(15) (a) Duriska, M. B.; Neville, S. M.; Moubaraki, B.; Cashion, J. D.; Halder, G. J.; Chapman, K. W.; Balde, C.; Letard, J.-F.; Murray, K. S.; Kepert, C. J.; Batten, S. R. *Angew. Chem., Int. Ed.* **2009**, *48*, 2549–2552. (b) Lu, Z.; Knobler, C. B.; Furukawa, H.; Wang, B.; Liu, G.; Yaghi, O. M. *J. Am. Chem. Soc.* **2009**, *131*, 12532–12533. (c) Ghosh, K.; Hu, J.; White, H. S.; Stang, P. J. *J. Am. Chem. Soc.* **2009**, *131*, 6695–6697. (d) Oppel, I. M.; Foecker, K. *Angew. Chem., Int. Ed.* **2008**, *47*, 402–405.

Scheme 2. Synthesis of Flexible Dipyrazolate Linkers

R=Ph; **a**	H_2L^1
Me; **b**	H_2L^2
Me; **c**	H_2L^3
Ph; **d**	H_2L^4
Me; **e**	H_2L^5
Ph; **f**	H_2L^6
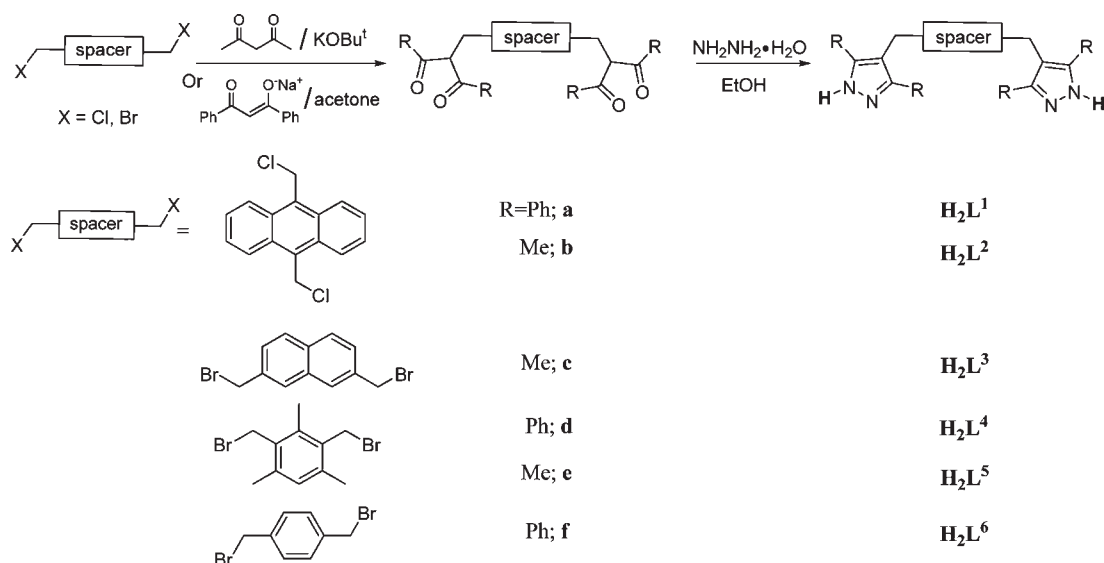
important role in both inorganic and organometallic chemistry, which have been rarely reported.[18] In the past years, we have been interested in developing the emerging supramolecular self-assembly via metal−metal bonding or bonding interaction.[19] In our previous work, we have developed the solution self-assembly method and structural characterization of a series of metallomacrocyclic complexes with dipalladium (II, II) and diplatinum (II, II) centers and multipyrazolate anion linkers via spontaneous deprotonation in aqueous solution.[20−22]

Herein, we designed the flexible dipyrazolyl ligands with luminescent spacers. With anthracene-based dipyrazolate dianion as the linker and $[(bpy)_2Pd_2(NO_3)_2](NO_3)_2$ or $[(phen)_2Pd_2(NO_3)_2](NO_3)_2$ dimetallic clips as the corner, we synthesized and characterized a series of metallomacrocyclic complexes with interior cavities via self-assembly in aqueous solution (as shown in Scheme 1). Host−guest properties for luminescent metal macrocyclic

host and aromatic guests (depicted in Chart 1) were studied though UV−vis and fluorescent titrations.

Results and Discussion

Self-Assembly and Characterization of the $[M_4L_2]^{4+}$-Type Metallomacrocycles. $[(bpy)_2Pd_2(NO_3)_2](NO_3)_2$ or $[(phen)_2Pd_2(NO_3)_2](NO_3)_2$ was treated with a solution containing 0.5 equivalent of H_2L^n (*n* labeled by 1, 2, 3, 4, 5, 6) (as shown in Scheme 2) in water at room temperature over 2 h, followed by adding acetone into the solution. The resulting mixture was heated at 60 °C for 12 h to produce $[M_4L_2]$-$(NO_3)_4$ in quantitative yield with spontaneous deprotonation of dipyrazole ligands. The ^1H and ^{13}C NMR analyses of the product indicated the formation of a single highly symmetrical species, and integration of the signals is indicative of 2:1 ratio of metal complex ($(bpy)Pd^{2+}$ or $(phen)Pd^{2+}$) fragment to the dipyrazolate dianion.

The formation of the $[M_4L_2]^{4+}$-type metallomacrocyclic structure is further supported by electrospray ionization mass spectrometry (ESI-MS). For the hexafluorophosphate complex, the ESI-MS experiment was performed in acetonitrile solution. As shown in Figure 1a, the signals at $m/z = 1310.2$, 825.5, and 583.1, which are assignable to $[1 \cdot 2PF_6^-]^{2+}$, $[1 \cdot PF_6^-]^{3+}$, and $[1]^{4+}$, respectively. In Figure 1b, 1062.1, 660.1, and 458.8 are assignable to $[3 \cdot 2PF_6^-]^{2+}$, $[3 \cdot PF_6^-]^{3+}$, and $[3]^{4+}$, respectively.

Self-Assembly and Characterization of $[M_8L_4]^{8+}$-Type Metallomacrocycle. Unlike other flexible dipyrazolate ligands, the treatment of H_2L^1 with $[(phen)_2Pd_2(NO_3)_2]$-$(NO_3)_2$ in a 1:2 ratio in water and acetone quantitatively gave the metallomacrocycles complex $\{[(phen)Pd]_8L^1_4\}$-$(NO_3)_8$ instead of $[M_4L_2]^{4+}$, which resulted in a huge metallomacrocyle with a big cavity, as shown in Scheme 3.

The assignment of $[M_8L_4]^{8+}$-type metallomacrocycle $9 \cdot 8PF_6^-$ is proved by ESI-MS studies, as shown in Figure 2. The multiple-charged molecular ions of $9 \cdot 8PF_6^-$ at $m/z = 1058.1$, 857.8, 714.4, and 607.1 are ascribed to $[9 \cdot 3PF_6^-]^{5+}$, $[9 \cdot 2PF_6^-]^{6+}$, $[9 \cdot 1PF_6^-]^{7+}$, and $[9]^{8+}$, respectively.

Ring numbers of cyclic assemblies are often controlled by changing reaction conditions (concentration, temperature, etc.) or by adding a template molecule that selectively binds to and stabilizes one particular assembly. In this

(16) (a) Iengo, E.; Milani, B.; Zangrando, E.; Geremia, S.; Alessio, E. *Angew. Chem., Int. Ed.* **2000**, *39*, 1096–1099. (b) Drain, C. M.; Nifiatis, F.; Vasenko, A.; Batteas, J. D. *Angew. Chem., Int. Ed.* **1998**, *37*, 2344–2347. (c) Funatsu, K.; Imamura, T.; Ichimura, A.; Sasaki, Y. *Inorg. Chem.* **1998**, *37*, 1798–1804. (d) Slone, R. V.; Hupp, J. T. *Inorg. Chem.* **1997**, *36*, 5422–5423. (e) Drain, C. M.; Lehn, J.-M. *J. Chem. Soc., Chem. Commun.* **1994**, *19*, 2313–2315.

(17) (a) Yu, S.-Y.; Huang, H.; Liu, H.-B.; Chen, Z.-N.; Zhang, R.; Fujita, M. *Angew. Chem., Int. Ed.* **2003**, *42*, 686–690. (b) Li, S.-H.; Huang, H.-P.; Yu, S.-Y.; Li, Y.-Z.; Huang, H.; Sei, Y.; Yamaguchi, K. *Dalton Trans.* **2005**, 2346–2348. (c) Liu, L.-X.; Huang, H.-P.; Li, X.; Sun, Q.-F.; Sun, C.-R.; Li, Y.-Z.; Yu, S.-Y. *Dalton Trans.* **2008**, 1544–1545. (d) Ning, G.-H.; Xie, T.-Z.; Pan, Y.-J.; Li, Y.-Z.; Yu, S.-Y. *Dalton Trans.* **2010**, 3203–3211.

(18) Cotton, F. A., Murillo, C. A., Walton, R. A. *Multiple Bonds between Metal Atoms*, 3rd ed.; Springer Science and Business Media: New York, 2005.

(19) (a) Yu, S.-Y.; Sun, Q.-F.; Lee, T. K.-M.; Cheng, E. C.-C.; Li, Y.-Z.; Yam, V. W.-W. *Angew. Chem., Int. Ed.* **2008**, *24*, 4551–4554. (b) Sun, Q.-F.; Lee, T. K.-M.; Li, P.-Z.; Yao, L.-Y.; Huang, J.-J.; Huang, J.; Yu, S.-Y.; Li, Y.-Z.; Cheng., E. C. -C.; Yam, V. W.-W. *Chem. Commun.* **2008**, *43*, 5514–5516. (c) Yu, S.-Y.; Zhang, Z.-X.; Cheng, E. C.-C.; Li, Y.-Z.; Yam, V. W.-W.; Huang, H.-P.; Zhang, R. *J. Am. Chem. Soc.* **2005**, *127*, 17944–17995. (d) Cotton, F. A.; Lei, P.; Lin, C.; Murillo, C. A.; Wang, X.-P.; Yu, S.-Y.; Zhang, Z.-X. *J. Am. Chem. Soc.* **2004**, *126*, 1518–1525.

(20) Yu, S.-Y.; Jiao, Q.; Li, S. H.; Huang, H. P.; Li, Y. Z.; Pan, Y. J.; Yamaguchi, K. *Org. Lett.* **2007**, *9*, 1379–1382.

(21) (a) Yu, S.-Y.; Huang, H. P.; Li, S. H.; Jiao, Q.; Li, Y. Z.; Wu, B.; Sei, Y.; Yamguchi, K.; Pan, Y. J.; Ma, H. W. *Inorg. Chem.* **2005**, *44*, 9471–9488. (b) Li, S. H.; Huang, H. P.; Yu, S.-Y.; Li, X.-P. *Chin. J. Chem.* **2006**, *24*, 1225–1229.

(22) Sun, Q. F.; Liu, L. X.; Huang, H. P.; Yu, S.-Y.; Yam, W. W. V. *Inorg. Chem.* **2008**, *47*, 2142–2145.
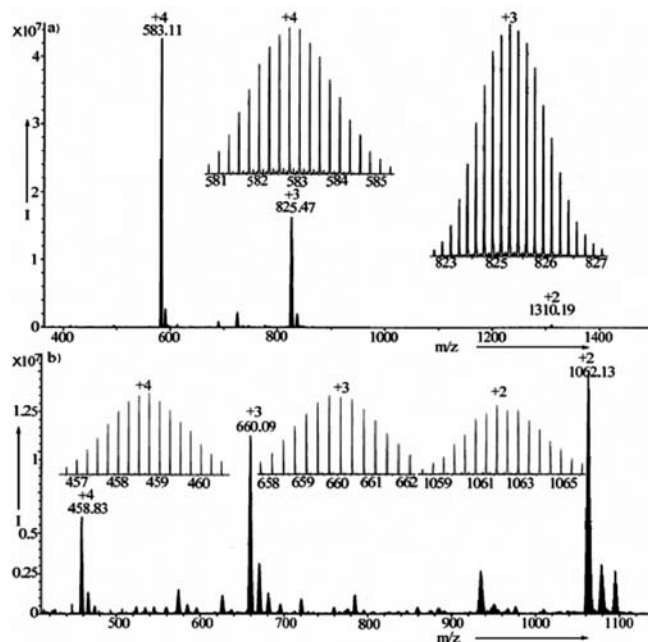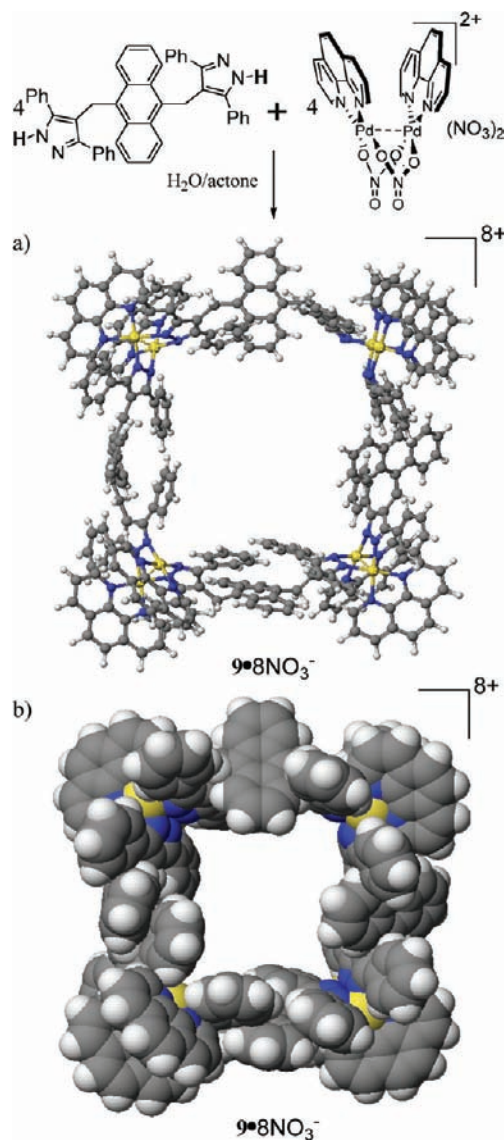
Figure 1. ESI-MS spectra of (a) **1**·4PF$_6^-$ and (b) **3**·4PF$_6^-$ in acetonitrile. The inset shows the isotopic distribution of the species (a) $[1 \cdot PF_6^-]^{3+}$ and $[1]^{4+}$ and (b) $[3 \cdot 2PF_6^-]^{2+}$, $[3 \cdot PF_6^-]^{3+}$, and $[3]^{4+}$.

Scheme 3. Self-Assembly and Top View of Macrocycle **9**·8NO$_3^-$ Calculated with CACHe 6.1.1 Program (see ref 30)[a]

^{a} (a) Ball-and-stick model and (b) Space-and-stack model. (yellow: Pd; gray: C; white: H; and blue: N).

work, to control the size of the metallomacrocycle, we used the dimetallic clips with a rigid phen ring, which could produce more hindrance than the bpy ligand.

Crystal Structure of Assembly $[M_4L_2]^{4+}$-Type Metallomacrocycles. The ORTEP diagram of **1**·4PF$_6^-$ is shown in Figure 3. Complex **1**·4PF$_6$ crystallizes in the orthorhombic space group *Fddd*. The crystal structure analysis for **1**·4PF$_6^-$ reveals the Pd$_4$ bowl-shaped macrocyclic structure with two (μ-pyrazolato-N,N')$_2$ doubly bridged [(bpy)Pd]$_2$ dimetal corners. The two anthracene rings form a dihedral angle of 90 °, and each one forms a dihedral angle of about 60.9 and 71.8° with *pz* planes in the dipyrazole bridged ligand. The Pd1···Pd2 separation of 3.157 Å suggests the presence of weak metal−metal interaction. The dihedral angles between the two *pz* (N3A−N4A and N1A−N2A; N4-−N3 and N1−N2) planes at each corner are 89.25 and 70.50°, which are smaller than the dihedral angles between the Pd1A−N3A−N4A−Pd2A and Pd1−N3−N4−Pd2 planes (116.38 and 115.05°). The cavity of the Pd$_4$ bowl-shaped macrocycle is small, because it is twisted by the two vertical anthracene planes. The distances of Pd1−Pd1A and Pd2−Pd2A are 11.95 and 13.32 Å, respectively.

The ORTEP diagram of **3**·4PF$_6^-$·8CH$_3$CN·H$_2$O is shown in Figure 4. Complex **3**·4PF$_6^-$ crystallizes in the monoclinic space group *C2/c* with one cocrystallized water molecule. The crystal structure analysis for **3**·4PF$_6^-$ reveals the Pd$_4$ bowl-shaped macrocyclic structure with two (μ-pyrazolato-N,N')$_2$ doubly bridged [(bpy)Pd]$_2$ dimetal corners. The two anthracene rings each form a dihedral angle of about 80° with *pz* planes in the dipyrazole bridged ligand, showing a syn−syn orientation according to the planes of (bpy)Pd1A and (bpy)Pd1B. The Pd1A···Pd2A separation of 3.232 Å suggests the presence of weak metal−metal interactions. The remarkable structure feature is that the (bpy)Pd1A and (bpy)Pd2A planes (with a dihedral angle of 82.4°) form a cleft with a cavity size of approximately 7.09 Å (center-to-center distance). As shown

in Figure 4b, one CH$_3$CN binds between the two bpy rings by C−H···π interactions between the H54A atom and X (1D) (the centroid of one bpy ring), which is separated by 2.565 Å (C54A−H54A···π) with the C−H···X angle 158.11°. Furthermore, two acetonitrile molecules are encapsulated through C−H···π interactions[22] within the aromatic ring built cavity, and the distances from C−H of the CH$_3$CN to the three centroids (X (1A), X (1B), X (1C) in Figure 4a of the three adjacent aromatic planes are 3.067, 3.052, and 2.672 Å with the C−H···X angles 140.90, 153.35, and 132.54°, respectively. Similarly short intermolecular C−H···π distances were previously found between CH$_3$ and an aromatic ring (2.75, 2.89 Å).[23a,c] The inclusion

(23) (a) Nishio, M.; Umezawa, Y.; Honda, K.; Tsuboyama, S.; Suezawa, H. *CrystEngComm* **2009**, *11*, 1757. (b) Nishio, M. *CrystEngComm* **2004**, *6*, 130. (c) Nishio, N.; Hirota, M.; Umezawa, Y. *The CH/π Interaction. Evidence, Nature, and Consequences*. Wiley-VCH, New York, 1998. (d) Kishikawa, K.; Yoshizaki, K.; Kohmoto, S.; Yamamoto, M.; Yamaguchi, K.; Yamada, K. *J. Chem. Soc., Perkin Trans. 1* **1997**, 1233.
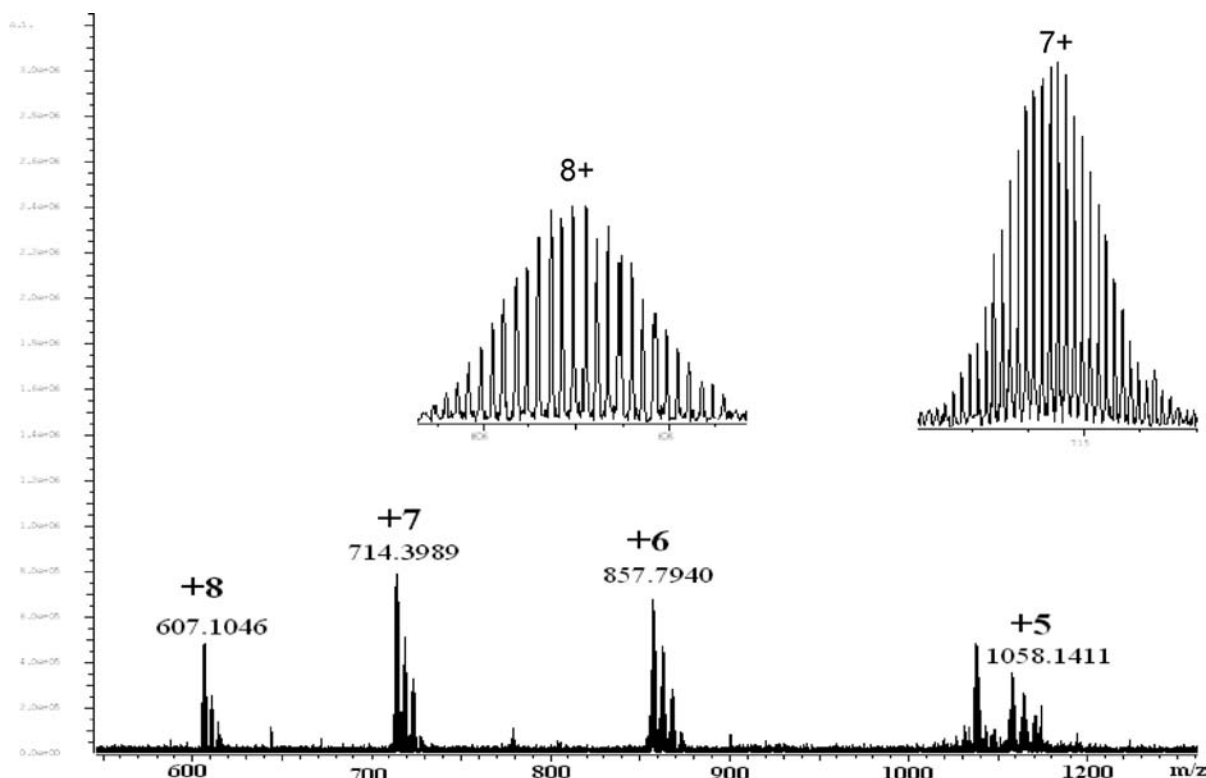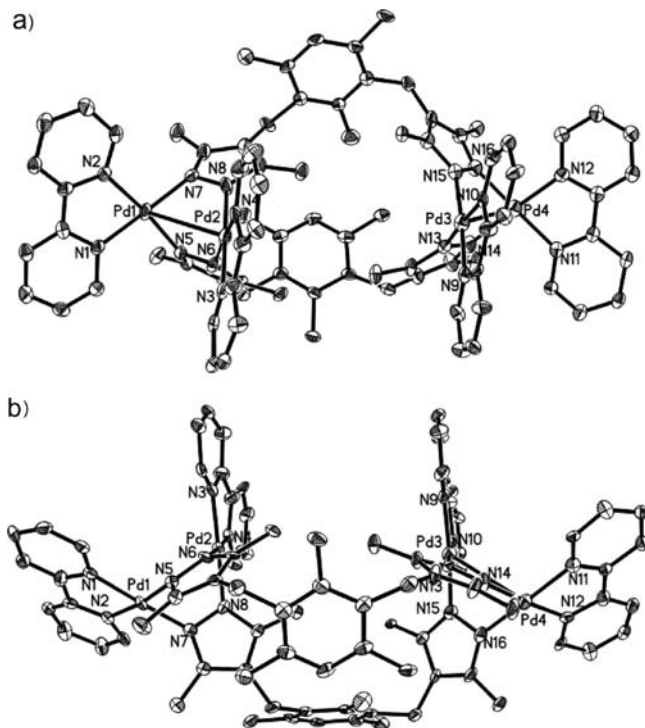
Figure 2. ESI-MS spectra of **9**·8PF$_6^-$ in acetonitrile. The inset shows the isotopic distribution of the species [**9**·PF$_6^-$]$^{7+}$ and [**9**]$^{8+}$.
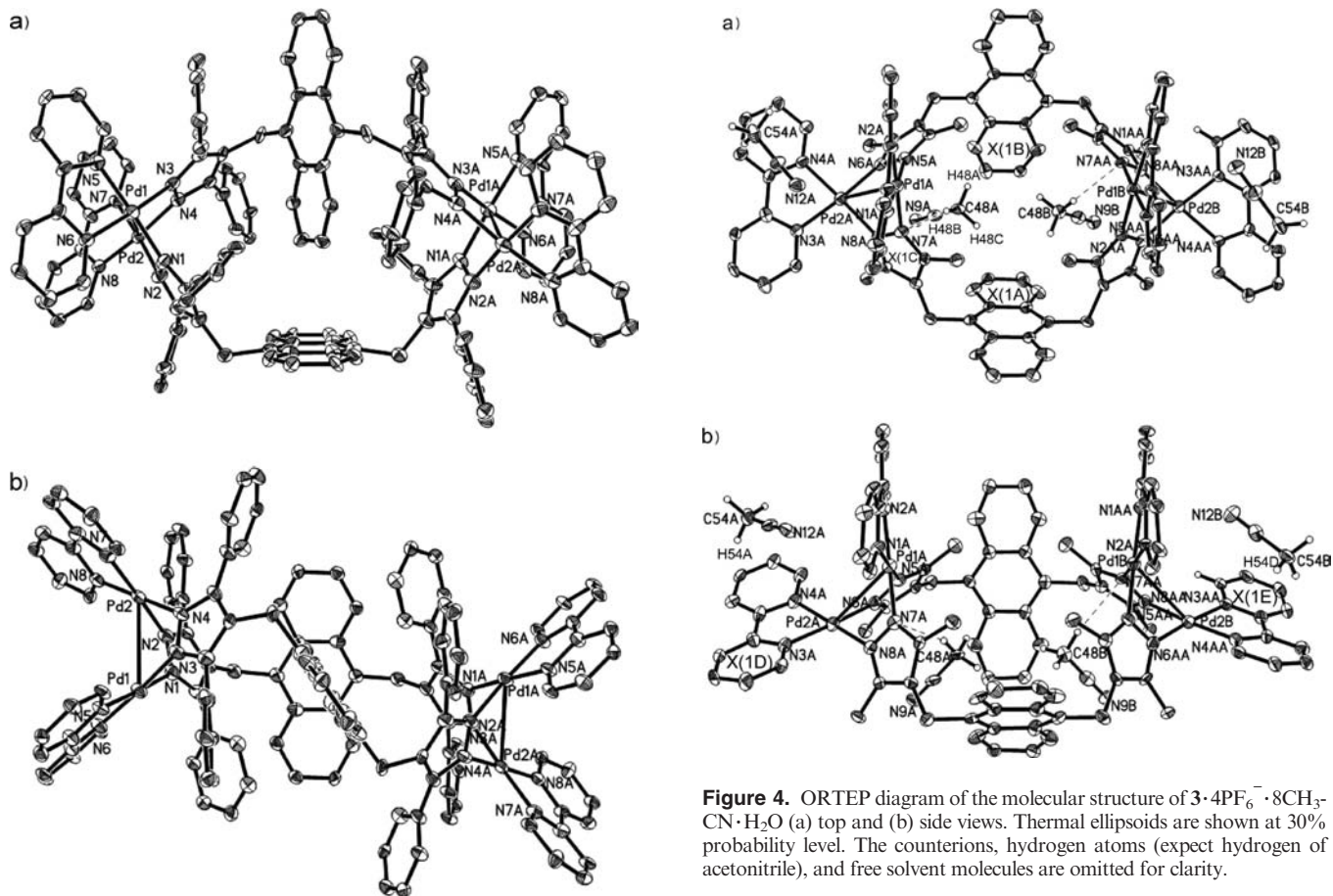
Figure 3. ORTEP diagram of the molecular structure of **1**·4PF$_6^-$ (a) top and (b) side views. Thermal ellipsoids are shown at 30% probability level. The counterions, hydrogen atoms, and solvent molecules are omitted for clarity.

Figure 4. ORTEP diagram of the molecular structure of **3**·4PF$_6^-$·8CH$_3$-CN·H$_2$O (a) top and (b) side views. Thermal ellipsoids are shown at 30% probability level. The counterions, hydrogen atoms (expect hydrogen of acetonitrile), and free solvent molecules are omitted for clarity.

tropism is opposite to the case of CH$_3$CN entrapped within the (V$_{12}$O$_{32}$$^{4-}$) inorganic bowl,[24] whereas the cyanogen was inward. The cavity of the Pd$_4$ bowl-shaped macrocycle is

a)

b)

Figure 5. ORTEP diagram of the molecular structure of **7**·4PF$_6^-$·6H$_2$O (a) top and (b) side views. Thermal ellipsoids are shown at 30% probability level. The counterions, hydrogen atoms, and solvent molecules are omitted for clarity.

small. The distance between the two central anthracene rings is 8.1 Å, and the distances of Pd1A−Pd1B and Pd2A−Pd2B are 8.59 and 12.85 Å, respectively.

The ORTEP diagram of **7**·4PF$_6^-$·6H$_2$O is shown in Figure 5. Complex **7**·4PF$_6^-$ crystallizes in the monoclinic space group $P2_1/c$. The crystal structure analysis for **7**·4PF$_6^-$ reveals the Pd$_4$ bowl-shaped macrocyclic structure with two (μ-pyrazolato-N,N')$_2$ doubly bridged [(bpy)Pd]$_2$ dimetal corners. The two benzene rings form a dihedral angle of 56.18° and form dihedral angles of about 85.09, 85.43° and 83.95, 87.24° with pz planes in the bipyrazole bridged ligand, showing a syn−syn orientation according to the planes of (bpy)Pd1 and (bpy)Pd3. The Pd1···Pd2 separation of 3.232 Å suggests the presence of weak metal−metal interactions. The dihedral angles between the two pz (N7−N8 and N5−N6; N13−N14 and N15−N16) planes at each corner are 58.34 and 87.31°, which are smaller than the dihedral angles between the Pd1−N7−N8−Pd2 and Pd3−N13−N14−Pd4 planes (117.77 and 118.76°). The cavity of the Pd$_4$ bowl-shaped macrocycle is small because the four pyrazole methyl groups fill in the cavity. The distances of Pd1−Pd4 and Pd2−Pd3 are 12.685 and 7.823 Å, respectively.

UV−vis Titrations and Fluorescent Spectra. The **H$_2$L^1** has been synthesized in high yields (Scheme 1). In dimethyl sulfoxide (DMSO), it exhibited characteristic anthracene emission and fluorescence maxima at 421, 440, and 465 nm and UV−vis spectrum peaks at 405, 382, 364, and 346 nm, respectively (Supporting Information, Figure 1S). When the [(bpy)$_2$Pd$_2$(NO$_3$)$_2$](NO$_3$)$_2$ was added into **H$_2$L^1**, the

Table 1. Summary of the Association Constants of the New Metallomacrocycle−Aromatic Guest Complexes Determined by UV-vis Titration Method

complex	K_a (M^{-1})
1·Dmb	1.42×10^6
1·Dhb	1.11×10^5
1·An	2.7×10^5
1·Ben-CO$_2^-$Na$^+$	3.48×10^5
1·Py	a
1·Hfb	a

^{a} Cannot be determined because the change of absorbance does not linearly relate to [G].

emission intensity of **H$_2$L^1** in fluorescent spectra was quenched sharply, and the absorbance of **H$_2$L^1** in UV−vis spectra was decreased notably (Supporting Information, Figure 1S), due to the coordination between the N atom of pyrazole and the Pd atom and the distortion effects on the emission quantum yield (Φ_{em}) of the anthracenyl rings.

Upon addition of aromatic guests to the solution of the receptors in DMSO, the absorbance of the receptors in the UV−vis spectrum was shifted significantly. Figure 7a presented the UV−vis spectra of **1** in DMSO in the presence of an incremental amount of Dmb. (Dhb, An, and Ben-CO$_2^-$Na$^+$ are shown in Supporting Information, Figures 6S−8S, respectively.) Job's plot analysis based on the UV−vis experiments, as shown in Supporting Information, Figures 2S−5S, supported a 1:1 stoichiometry for complexes **1**:Dmb, **1**:Dhb, **1**:An, and **1**: Ben-CO$_2^-$Na$^+$, which exhibited the largest change of absorbance at the 1:1 ratio of the receptor and the aromatic guests when the total concentration of the two samples was kept constant.[25,26]
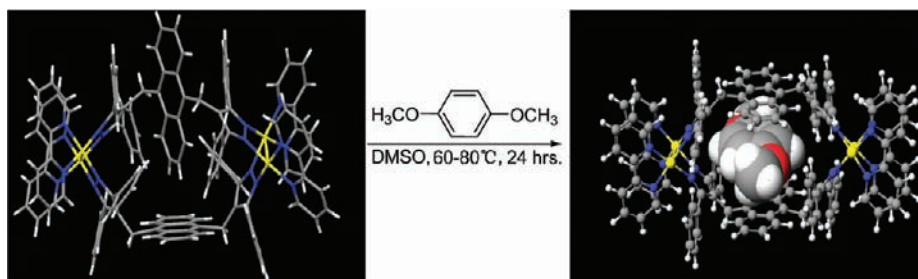
The association constants (K_a) of complexes **1**·Dmb, **1**·Dhb, **1**·An, and **1**·Ben-CO$_2^-$Na$^+$ in DMSO were then evaluated by the UV−vis titration method. On the basis of the change values of absorbance with (aromatic guests), we estimated the K_a of the four complexes to be 1.42×10^6, 1.11×10^5, 2.7×10^5, and 3.48×10^5 M^{-1}, respectively (Table 1). Fluorescence studies (Figure 7b) revealed that the emission intensity of the anthracene ring units of the receptors could be significantly increased by the aromatic guest (Dhb, An, and Ben-CO$_2^-$Na$^+$ are shown in Supporting Information, Figures 9S−11S, respectively). These results are consistent with the above UV−vis investigation, reflecting the remarkably complexing affinity between the two anthracene rings of **1** and the aromatic guest due to the $\pi-\pi$ stacking interactions (Figure 6).

Such similar spectroscopic changes were not observed when an incremental amount of Hfb and Py were added to the solution of **1** in DMSO as well as An, Hfb, and Ben-CO$_2^-$Na$^+$ were added to the solution of **3** in DMSO, which may be rationalized by considering steric hindrance and electrostatic repulsion. The cavity of host **1** is too small to include the Py, and Hfb is an electron-defect compound which is unfavorable for binding with the positively charged metallomacrocycle **1**. There are
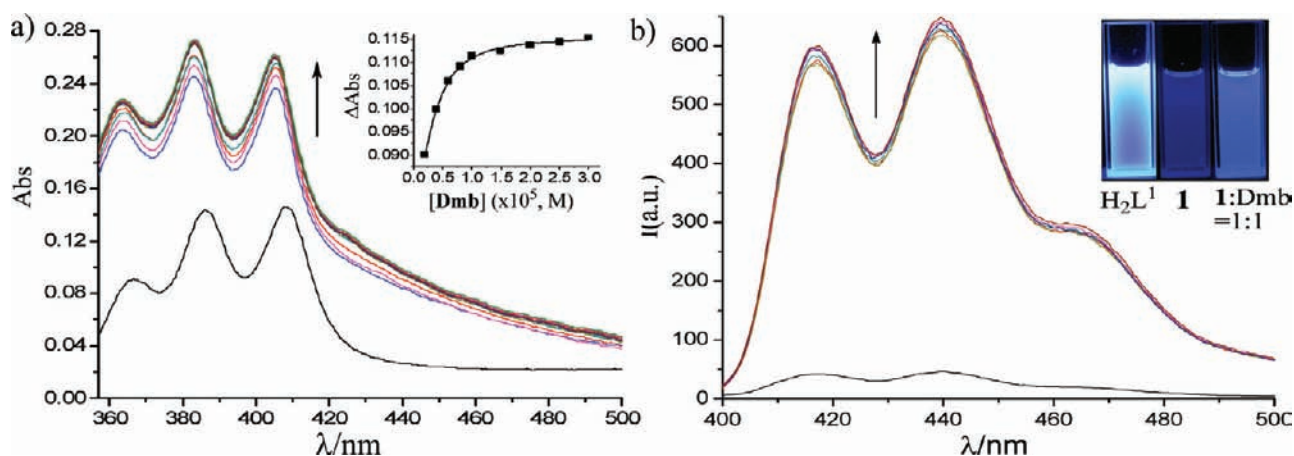
(24) Day, V. W.; Klemperer, W. G.; Yaghi, O. M. *J. Am. Chem. Soc.* **1989,** *111,* 5959−5961.

(25) (a) Schneider, H. J.; Yatasimirsky, A. *Principle and Methods in Supramolecular Chemistry,* Wiley: New York, 2000. (b) Conners, K. A. *Binding Constants: The Measurement of Molecular Complex Stability,* Wiley: New York, 1987.

(26) Li, W. S.; Jiang, D. L.; Suna, Y.; Aida, T. *J. Am. Chem. Soc.* **2005,** *127,* 7700−7702.

Figure 6. Possible mechanism for host−guest interaction. Left, crystal structure of **1** and right, 1:1 complex Dmb·**1** calculated with CAChe 6.1.1 program[30] (yellow: Pd; gray: C; white: H; and blue: N).

Figure 7. (a) Absorption spectral changes of **1** (1×10^{-5} M) upon addition of Dmb in DMSO at 25 °C (black is the UV−vis absorbance of **1**, and inset is the plot of the absorbance change vs [Dmb], at peak of 406 nm). (b) Changes in emission spectra of **1** (1×10^{-5} M) upon addition of Dmb in DMSO (the inset shows the color difference for visual observation of the emission intensities, at $\lambda_{ex} = 365$ nm, of **H_2L^1** (2×10^{-5} M), **1** (1×10^{-5} M), and Dmb·**1** = 1:1 in DMSO).

Table 2. Crystallographic Data for Complexes **1**, **3**, and **7**

	1·4PF$_6^-$	**3**·4PF$_6^-$·8CH$_3$CN·H$_2$O	**7**·4PF$_6^-$·6H$_2$O
formula	$C_{132}H_{96}N_{16}F_{24}P_4Pd_4$	$C_{108}H_{106}F_{24}N_{24}OP_4Pd_4$	$C_{82}H_{96}F_{24}N_{16}O_6P_4Pd_4$
FW	2911.73	2761.65	2407.23
crystal size [mm]	0.20 × 0.22 × 0.24	0.22 × 0.24 × 0.28	0.20 × 0.22 × 0.26
crystal system	orthorhombic	monoclinic	monoclinic
space group	*Fddd*	*C2/c*	*P2$_1$/c*
a [Å]	44.0262(10)	38.8468(8)	21.483(10)
b [Å]	22.4503(5)	12.6578(2)	18.296(8)
c [Å]	71.5704(16)	25.2201(4)	30.191(14)
α [°]	90	90	90
β [°]	90	103.034(1)	100.777(6)
γ [°]	90	90	90
V [Å^3]	70 740(3)	12 081.6(4)	11 657(9)
Z	16	4	4
ρ_{calcd}, [g/cm^{-3}]	1.094	1.518	1.372
μ [mm^{-1}]	0.502	0.733	0.749
$F(000)$	23 360	5560	4832
$2\theta_{max}$ [°]	50.00	52.00	52.00
no. unique data	15 599	11 874	22 867
parameters	811	752	1320
GOF [F^2]^a	1.02	1.05	1.09
R [$F^2 > 2\sigma(F^2)$], $wR[F^2]^b$	0.0488, 0.0934	0.0495, 0.1338	0.0514, 0.1379
$\Delta\rho_{max}$, $\Delta\rho_{min}$ [e Å^{-3}]	−0.32, 0.64	−0.58, 0.35	−0.65, 0.33

^{a} GOF $= [w(F_o^2 - F_c^2)^2]/(n - p)^{1/2}$, where n and p denote the number of data points and parameters, respectively. ^{b} R1 $= (\|F_o| - |F_c\|)/|F_o|$; wR2 $= [w(F_o^2 - F_c^2)^2]/[w(F_o^2)^2]^{1/2}$, where $w = 1/[\sigma^2(F_o^2) + (aP)^2 + bP]$ and $P = [\max(0, F_o^2) + 2F_c^2]/3$.

four methyl groups filling the small cavity of **3**, which keeps the aromatic guests outside the cavity.

Conclusions

Fluorescent dipyrazolate-bridged metallomacrocycles with dipalladium(II, II) centers can be obtained in nearly quantitative yield from [(bpy)$_2$Pd$_2$(NO$_3$)$_2$](NO$_3$)$_2$ or [(phen)$_2$-Pd$_2$(NO$_3$)$_2$](NO$_3$)$_2$ and 1H-bipyrazolyl ligands in a 2:1 molar ratio via a directed self-assembly process that occurs along with spontaneous deprotonation of the ligands. Ring size and shape of cyclic assemblies {[M$_4$L$_2$](NO$_3$)$_4$ and [M$_8$L$_4$](NO$_3$)$_8$} have been controlled by fine-tuning different dimetallic clips

and flexible dipyrazole ligands. The assemblies have been characterized by elemental analysis, ^{1}H and ^{13}C NMR, electrospray ionization mass spectrometry (ESI-MS), and single crystal X-ray diffraction methods for **1**, **3**, and **7**. In addition, the 1:1 host−guest complexation for the anthracene-based dipyrazolate-bridged macrocycle (**1** and **3**) with aromatic guests was investigated via UV−vis and fluorescence spectra.

Experimental Section

Materials. All chemicals and solvents were of reagent grade and were purified according to conventional methods.[27] The dimetal clips [(bpy)$_2$Pd$_2$(NO$_3$)$_2$](NO$_3$)$_2$ and [(phen)$_2$Pd$_2$(NO$_3$)$_2$]-(NO$_3$)$_2$ were prepared according to literature procedures.[28,29]

X-ray Structural Determinations. X-ray diffraction measurements were carried out at 291 K on a Bruker Smart Apex CCD area detector equipped with a graphite monochromated Mo Kα radiation (λ = 0.71073 Å). The absorption correction for all complexes was performed using SADABS. All the structures were solved by direct methods and refined employing full-matrix least-squares on F2 by using the SHELXTL (Bruker, 2000) program and were expanded using Fourier techniques. All nonhydrogen atoms of the complexes were refined with anisotropic thermal parameters. The hydrogen atoms were included in idealized positions. Final residuals along with unit cell, space group, data collection, and refinement parameters are presented in Table 2.

Typical Procedures for the UV−vis Titration and Evaluation Constants K_a. Aliquots of a fixed solution of the aromatic guests in DMSO were added to a DMSO solution of the receptors (**1** and **3**), and the mixture was heated at 60 °C then cooled to 25 °C and subjected to the UV−vis spectroscopy. The spectrum was corrected with a dilution factor and background subtraction. The difference in absorbance (ΔAbs) of the receptors in the presence of the guest and the absence of the guest was recorded, and the data were plotted against [G]. The association constant K_a for the 1:1 complexes was derived by using the nonlinear curve fitting based on the equation:[25,26]

$$\Delta A = \Delta A \infty ((1 + K_a[G] + K_a[H]_0) - ((1 + K_a[G] + K_a[H]_0)^2 - 4K_a^2[H]_0[G])^{0.5})) / (2K_a[H]_0)$$

where $\Delta A = A - \Delta A_0$, $\Delta A \infty = A \infty - A_0$, [G] is concentration of aromatic guests, [H]$_0$ is [**1**·4NO$_3^-$].

CAChe Program 6.1.1. A visual molecular model was computed using the CAChe program 6.1.1[30] to evaluate shape of macrocycle **9** (Scheme 3) and the host−guest complex Dmb·**1** (Figure 6).

General Procedure for Bis(methylene)dipentane-2,4-dione Preparation[20]. Acetylacetone (1.81 g, 18.1 mmol) was added during a 30 min period to a stirred, refluxing solution prepared from potassium (706 mg, 18.1 mmol) and 60 mL of t-butyl alcohol. After 50 min, the solution of bis(bromomethyl) compound (8.23 mmol) in 30 mL of THF was added during a 30 min period, and 1 h after the addition, KI (10% quality of bis-(bromomethyl) compounds) was added. The resultant solution was stirred and heated at reflux temperature until acidic to moist litmus (ca. 16 h). After three-fourths of the solvent was distilled, the residue was washed with water and extracted with CH$_2$Cl$_2$. The organic phase was dried over anhydrous MgSO$_4$, and the

solvent and excess acetylacetone was distilled. Further purification was achieved by recrystallization or column chromatography, as noted below.

General Procedure for Bis(1,3-diphenylpropane-1,3-dione) Preparation. Bis(bromomethyl) (2 mmol), sodium 1,3-diphenyl-prop-1-en-1-olate (DBMNa) (4.4 mmol), and KI (10% of quality of bis(bromomethyl)) were mixed in a 250 mL round flask. Then 150 mL dry acetone was added under N$_2$ protection, the resulting solution was stirred and refluxed for 16 h. After cooling to room temperature, most of solvent was distilled. Then the residue was washed with water and extracted with CH$_2$Cl$_2$, the organic phase was dried over anhydrous MgSO$_4$ and filtered, and the solvent was distilled. Further purification was achieved by recrystallization or column chromatography, as noted below.

General Pyrazole Preparation. Hydrazine hydrate (1 mL, 80%) was added during a 10 min period to a stirred and refluxed solution of dione (1 mmol) in 30 mL of ethanol. After 12 h, most of the solvent was distilled and filtered, and the resulting solid was washed twice with water and vacuum dried.

2,2′-(Anthracene-9,10-diylbis(methylene))bis(1,3-diphenylpropane-1,3-dione) (a). The above general bis(1,3-diphenylpropane-1,3-dione) preparation procedure was followed with 9,10-bis-(chloromethyl)anthracene (550 mg, 2 mmol) to give **a** as a light-yellow powder. The rough product was washed twice with hot 50 mL ethanol and vacuum dried. (1.17 g, 90%). ^{1}H NMR (400 MHz, CDCl$_3$, 25 °C, ppm): δ = 8.08−8.06 (m, 4H), 7.47−7.45 (m, 8H), 7.36−7.34 (m, 4H), 7.31−7.28 (m, 4H), 7.09−7.05 (m, 8H), 5.61−5.57 (t, J = 2.84 Hz, 2H), 4.41−4.40 (s, J = 2.84 Hz, 4H). ^{13}C NMR (100 MHz, CDCl$_3$, 25 °C, ppm): δ = 196.2, 135.8, 133.2, 130.6, 129.6, 128.3, 128.2, 125.5, 124.8, 57.5, 27.3. MS (EI) m/z: Anal. calcd for [C$_{46}$H$_{34}$O$_4$ + Na]$^+$, 673.2349; found: 673.2344.

9,10-bis((3,5-Diphenyl-1H-pyrazol-4-yl)methyl)anthracene (H$_2$L^1). The above general pyrazole preparation procedure was followed with **a** (715 mg, 1.1 mmol) and a yellow solid H$_2$L^1 was obtained. (672 mg, 95%). ^{1}H NMR (400 MHz, DMSO-d_6, 25 °C, ppm): δ = 12.7 (s, 2H), 7.85−7.83 (m, 4H), 7.38 (2, 4H), 7.18−7.10 (m, 10H), 6.91−6.65 (m, 10H), 4.80(s, 4H). ^{13}C NMR (100 MHz, DMSO-d_6, 25 °C, ppm): δ = 130.9, 129.4, 128.1, 127.3, 127.0, 125.0, 124.0, 114.7, 23.3. Mass spectrometry (MS) Mtrix-assisted laser-desorption ionization (MALDI-TOF) coupled cluster approximation (CCA) (+) m/z: Anal. calcd for [C$_{46}$H$_{34}$N$_4$ + H]$^+$, 643.2856; found: 643.2859.

3,3′-(Anthracene-9,10-diylbis(methylene))dipentane-2,4-dione (b). 9,10-Bis(chloromethyl)anthracene (2.75 g, 10 mmol) scattered in DMF was slowly added to sodium 2,4-pentanedionat (3.66 g, 30 mmol) in 120 mL dry DMF, then the reaction was stirred and heated at 80 °C overnight. The resulting solution was cooled and poured into 500 mL of ice water. The solution was extracted twice with CH$_2$Cl$_2$ (500 mL), washed with saturated NaCl, organic phase dried over anhydrous Na$_2$SO$_4$, filtered, and the solvent was distilled. Chromatography on silica gel elution with CH$_2$Cl$_2$ afforded the intermediate as a light-yellow powder **b** (829 mg, 20.4%). ^{1}H NMR (400 MHz, CDCl$_3$, 25 °C, ppm): δ = 8.20−8.18 (m, 4H), 7.56−7.54 (m, 4H), 4.23−4.17 (m, 6H), 1.95 (s, 12H). ^{13}C NMR (100 MHz, CDCl$_3$, 25 °C, ppm): δ = 203.8, 130.4, 129.4, 125.9, 124.8, 68.25, 30.5, 26.28. MS (EI) m/z: Anal. calcd for [C$_{26}$H$_{26}$O$_4$ + Na]$^+$, 425.1723; found: 425.1706.

9,10-Bis((3,5-dimethyl-1H-pyrazol-4-yl)methyl)anthracene (H$_2$L^2). The above general pyrazole preparation procedure was followed except for the substitution of hydrazine hydrate (2 mL, 80%) and the **b** (680 mg, 1.7 mmol) in 50 mL of ethanol. Then the yellow solid H$_2$L^2 was obtained. (635 mg, 95%). ^{1}H NMR (400 MHz, DMSO-d_6, 25 °C, ppm): δ = 8.27−8.25 (m, 4H), 7.50−7.47 (m, 4H), 4.68 (s, 4H), 1.62 (s,12H). ^{13}C NMR (100 MHz, DMSO-d_6, 25 °C, ppm): δ = 131.3, 129.7, 125.5, 125.2, 112.9, 22.62, 10.8. MS (MALDI-TOF) m/z: Anal. calcd for [C$_{26}$H$_{26}$N$_4$ + H]$^+$, 395.2230; found: 395.2233.

(27) Armarego, W. L. F.; Perrin, D. D. *Purification of Laboratory Chemicals*, 4th ed.; Butterworth Heinemann; Oxford, U.K., 1997.

(28) (a) Huang, H. P.; Li, S. H.; Yu, S.-Y.; Li, Y.-Z.; Jiao, Q.; Pan, Y.-J. *Inorg. Chem. Commun.* **2005**, *8*, 656−660. (b) Yu, S.-Y.; Fujita, M.; Yamaguchi, K. *J. Chem. Soc., Dalton. Trans.* **2001**, 3145−3416.

(29) Conrad, R. C.; Rund, J. V. *Inorg. Chem.* **1972**, *11*, 129−134.

(30) *CAChe 6.1.1 for Windows*; Fujitsu Ltd.: Chiba, Japan, 2003.

2,7-Bis((3,5-dimethyl-1H-pyrazol-4-yl)methyl)naphthalene (H$_2$L^3). The above general pyrazole preparation procedure was followed with **c**[31] (250 mg, 0.71 mmol), and a white solid H$_2$L^3 was obtained. (232 mg, 95%). ^{1}H NMR (400 MHz, DMSO-d_6, 25 °C, ppm): δ = 12.02 (s, 2H) 7.72–7.704 (d, J = 8.2 Hz, 2H), 7.47 (s, 2H), 7.18–7.17 (d, J = 1.2 Hz, 2H), 3.78 (s, 4H), 2.06 (s,12H). ^{13}C NMR (100 MHz, DMSO-d_6, 25 °C, ppm): δ = 139.1, 133.2, 129.9, 127.4, 126.4, 125.2, 113.1, 28.7, 10.7. MS (MALDI-TOF) m/z: Anal. calcd for [C$_{22}$H$_{24}$N$_4$ + H]$^+$, 345.2074; found: 345.2072.

3,3′-(2,4,6-Trimethyl-1,3-phenylene)bis(methylene)dipentane-2,4-dione (d). The above general bis(methylene)dipentane-2,4-dione preparation procedure was followed with 2,4-bis(bromo-methyl)-1,3,5-trimethylbenzene (2.5 g, 8.23 mmol) to give **e** as a white powder. Then the rough product was recrystallized from 95% EtOH, and the colorless needle crystal was obtained. (2.49 g, 90%). ^{1}H NMR (400 MHz, CDCl$_3$, 25 °C, ppm): δ = 6.78 (s, 1H), 3.86–3.83 (t, J = 7.32 Hz, 2H), 3.15–3.13 (d, J = 7.32 Hz, 4H), 2.16 (s, 6H) 2.14 (s, 3H), 2.01 (s, 12H). ^{13}C NMR (100 MHz, CDCl$_3$, 25 °C, ppm): δ = 203.9, 134.7, 134.6, 133.3, 130.9, 66.7, 30.1, 28.5, 20.1, 16.1. MS (EI) m/z: Anal. calcd for [C$_{21}$H$_{28}$O$_4$ + Na]$^+$, 367.1880; found: 367.1881.

4,4′-(2,4,6-Trimethyl-1,3-phenylene)bis(methylene)bis(3,5-di-methyl-1H-pyrazole) (H$_2$L^4). The above general pyrazole preparation procedure was followed with **d** (500 mg, 1.45 mmol), and the yellow solid H$_2$L^4 was obtained. (463 mg, 95%). ^{1}H NMR (400 MHz, DMSO-d_6, 25 °C, ppm): δ = 12.80 (s, 2H), 7.31–6.96 (m, 20H), 6.24 (s, 1H), 3.71 (s, 4H), 1.73 (s, 6H), 1.36 (s, 3H). ^{13}C NMR (100 MHz, DMSO-d_6, 25 °C, ppm): δ = 135.1, 134.4, 133.4, 129.2, 128.4, 127.6, 127.1, 113.2, 25.0, 19.9, 16.1. MS (MALDI-TOF) m/z: Anal. calcd for [C$_{21}$H$_{28}$N$_4$ + Na]$^+$, 359.2206; found: 359.2198.

2,2′-(2,4,6-Trimethyl-1,3-phenylene)bis(methylene)bis(1,3-di-phenylpropane-1,3-dione) (e). The above general bis(1,3-diphenyl-propane-1,3-dione) preparation procedure was followed with 1,4-bis(bromomethyl)benzene (1 g, 4.11 mmol) to give **e** as a white solid. (2.31 g, 95%). ^{1}H NMR (400 MHz, CDCl$_3$, 25 °C, ppm): δ = 7.70–7.68 (m, 8H), 7.46–7.44 (m, 4H), 7.31–7.27 (m, 8H), 6.58 (s, 1H), 5.21–5.18 (t, J = 6.48 Hz, 2H), 3.46–3.44 (d, J = 6.48 Hz, 4H), 2.03 (s, 6H), 2.01 (s, 3H). ^{13}C NMR (100 MHz, CDCl$_3$, 25 °C, ppm): δ = 196.2, 136.0, 134.88, 134.82, 134.0, 133.3, 130.0, 128.5, 128.4, 57.3, 29.7, 20.2, 16.4. MS (EI) m/z: Anal. calcd for [C$_{41}$H$_{36}$O$_4$ + Na]$^+$, 615.2506; found: 615.2500.

4,4′-(2,4,6-Trimethyl-1,3-phenylene)bis(methylene)bis(3,5-di-phenyl-1H-pyrazole) (H$_2$L^5). The above general pyrazole preparation procedure was followed with **f** (500 mg, 0.60 mmol), and a white solid H$_2$L^5 was obtained. (468 mg, 95%). ^{1}H NMR (400 MHz, DMSO-d_6, 25 °C, ppm): δ = 12.80 (s, 2H) 7.31–7.15 (m, 16H), 6.96 (s, 4H), 6.24 (s, 1H), 3.71 (s, 4H), 1.73 (s, 6H), 1.36 (s, 3H). ^{13}C NMR (100 MHz, DMSO-d_6, 25 °C, ppm): δ = 135.1, 134.4, 133.4, 129.2, 128.4, 127.6, 127.1, 113.2, 25.0, 19.9, 16.1. MS (MALDI-TOF) m/z: Anal. calcd for [C$_{41}$H$_{36}$-N$_4$ + Na]$^+$, 607.2832; found: 607.2831.

2,2′-(1,4-Phenylenebis(methylene))bis(1,3-diphenylpropane-1,3-dione) (f). The above general bis(1,3-diphenylpropane-1,3-dione) preparation procedure was followed with 1,4-bis(bromo-methyl)benzene (500 mg, 1.89 mmol) to give **f** as a light-yellow powder. (1.00 g, 95%). ^{1}H NMR (400 MHz, CDCl$_3$, 25 °C, ppm): δ = 7.86–7.84 (m, 8H), 7.51–7.47 (m, 4H), 7.39–7.35 (m, 8H), 7.12 (s, 4H), 5.43–5.40 (t, J = 6.68 Hz, 2H), 3.37–3.35 (d, J = 6.64 Hz, 4H). ^{13}C NMR (100 MHz, CDCl$_3$, 25 °C, ppm): δ = 195.3, 137.4, 135.9, 133.4, 129.2, 128.8, 128.5, 58.9, 34.6. MS (EI) m/z: Anal. calcd for [C$_{38}$H$_{30}$O$_4$ + Na]$^+$, 573.2036; found: 573.2032.

1,4-Bis((3,5-diphenyl-1H-pyrazol-4-yl)methyl)benzene (H$_2$L^6). The above general pyrazole preparation procedure was followed

(31) Maverick, A. W.; Buckingham, S. C.; Yao, Q.; Bradbury, J. R.; Stanley, G. G. *J. Am. Chem. Soc.* **1986**, *108*, 7430–7431.

with **f** (200 mg, 0.36 mmol), and a white solid H$_2$L^6 was obtained. (187 mg, 95%). ^{1}H NMR (400 MHz, DMSO-d_6, 25 °C, ppm): δ = 13.33 (s, 2H) 7.46–7.32 (m, 20H), 6.98 (m, 4H), 4.00 (s, 4H). ^{13}C NMR (100 MHz, DMSO-d_6, 25 °C, ppm): δ = 138.4, 128.4, 127.8, 127.1, 111.8, 28.6. MS (MALDI-TOF) m/z: Anal. calcd for [C$_{38}$H$_{30}$N$_4$ + Na]$^+$, 565.2363; found: 565.2361.

Self-Assembly of Metalomacrocycles. General Procedures. **{[(phen)Pd]$_8$L$^1_4$}(NO$_3$)$_8$ (9·8NO$_3$$^-$).** [(phen)$_2Pd_2$(NO$_3$)$_2$](NO$_3$)$_2$ (41 mg, 0.1 mmol) was added to a suspension of H$_2$L^1 (32.2 mg, 0.05 mmol) in H$_2$O (10 mL), and the mixture was stirred for 2 h at room temperature. Then acetone (5 mL) was added, and the reaction was heated at 60 °C for 12 h at least. The resulting clear yellow solution was evaporated to dryness to give a yellow solid **1·8NO$_3$$^-$**. Yield: 69 mg (95%). The PF$_6$$^-$ salt of **9** was obtained as yellow microcrystals. ESI-MS (acetonitrile) m/z: 1058.1 [**9**·3PF$_6$$^-$]$^{5+}$, 857.8 [**9**·2PF$_6$$^-$]$^{6+}$, 714.4 [**9**·PF$_6$$^-$]$^{7+}$, 607.1 [**9**]$^{8+}$. Found: C, 54.50; H, 3.48; N, 7.19. Calcd for C$_{280}$H$_{192}$N$_{32}$-F$_{48}$P$_8$Pd$_8$·8H$_2$O (%): C, 54.59; H, 3.40; N, 7.28.

{[(bpy)Pd]$_4$L$^1_2$}(NO$_3$)$_4$ (1·4NO$_3$$^-$). The same procedure as employed for **9·8NO$_3$$^-$** was followed except that [(bpy)$_2$Pd$_2$-(NO$_3$)$_2$](NO$_3$)$_2$ (39 mg, 0.1 mmol) was used as the starting material. Yield: 58 mg (95%). The PF$_6$$^-$ salt of **1** was obtained as yellow microcrystals in quantitative yield. ^{13}C NMR (100 MHz, CD$_3$CN, 25 °C, ppm): δ = 207.8, 152.6, 152.4, 149.5, 149.2, 142.6, 142.1, 132.4, 129.3, 128.3, 127.6, 122.7, 83.2, 31.2, 25.9, 15.1. ESI-MS (acetonitrile) m/z: 1310.2 [**1**·2PF$_6$$^-$]$^{2+}$, 825.5 [**1**·PF$_6$$^-$]$^{3+}$, 583.1 [**1**]$^{4+}$. Found: C, 54.08; H, 3.40; N, 7.69. Calcd for C$_{132}$H$_{96}$N$_{16}$F$_{24}$P$_4$Pd$_4$·H$_2$O (%): C, 54.11; H, 3.37; N, 7.65. The single crystals suitable for X-ray determination were grown by the vapor diffusion of diethyl ether into a solution of **1·4PF$_6$$^-$** in acetonitrile at room temperature.

{[(phen)Pd]$_4$L$^2_2$}(NO$_3$)$_4$ (2·4NO$_3$$^-$). The same procedure as employed for **9·8NO$_3$$^-$** was followed except that H$_2$L^2 (19.7 mg, 0.05 mmol) was used as the starting material. Yield: 49 mg (80%). The PF$_6$$^-$ salt of **2** was obtained by adding a 10-fold excess of KPF$_6$ to its aqueous solution at 60 °C, which resulted in the immediate deposition of **2·4PF$_6$$^-$** as yellow microcrystals in quantitative yield. The crystals were filtered, washed with a minimum amount of cold water, and dried. ^{1}H NMR (400 MHz, CD$_3$CN, 25 °C, ppm) δ = 8.31–8.30 (m, 8H, phen-H$_{2,9}$), 8.13–8.11 (m, 8H, phen-H$_{4,7}$), 8.09 (s, 8H, phen-H$_{5,6}$), 7.93–7.90 (m, 8H, phen-H$_{3,8}$), 7.59–7.57 (m, 8H), 7.44–7.42 (m, 8H), 3.98 (s, 8H, L^2-CH$_2$), 2.44 (s, 24H, L^2-CH$_3$). ^{13}C NMR (100 MHz, CD$_3$CN, 25 °C, ppm): δ = 207.9, 153.1, 152.8, 152.5, 150.4, 148.7, 148.5, 142.7, 142.3, 132.2, 129.1, 128.7, 127.5, 123.2, 114.3, 82.2, 31.2, 26.2, 15.5. ESI-MS (acetonitrile) m/z: 1111.6 [**2**·2PF$_6$$^-$]$^{2+}$, 693.2 [**2**·PF$_6$$^-$]$^{3+}$, 483.3 [**2**]$^{4+}$. Found: C, 46.85; H, 3.33; N, 8.67. Calcd for C$_{100}$H$_{80}$N$_{16}$F$_{24}$P$_4$Pd$_4$·3H$_2$O (%): C, 46.82; H, 3.38; N, 8.74. Unfortunately the crystals were too small to collect the X-ray data.

{[(bpy)Pd]$_4$L$^2_2$}(NO$_3$)$_4$ (3·4NO$_3$$^-$). The same procedure as employed for **9·8NO$_3$$^-$** was followed except that [(bpy)$_2$Pd$_2$-(NO$_3$)$_2$](NO$_3$)$_2$ (39 mg, 0.1 mmol) and H$_2$L^2 (19.7 mg, 0.05 mmol) were used as the starting material. Yield: 55.7 mg (95%). The PF$_6$$^-$ salt of **3** was obtained by adding a 10-fold excess of KPF$_6$ to its aqueous solution at 60 °C, which resulted in the immediate deposition of **3·4PF$_6$$^-$** as yellow microcrystals in quantitative yield. The crystals were filtered, washed with a minimum amount of cold water, and dried. ESI-MS (aceto-nitrile) m/z: 1062.1 [**3**·2PF$_6$$^-$]$^{2+}$, 660.1 [**3**·PF$_6$$^-$]$^{3+}$, 458.8 [**3**]$^{4+}$. Found: C, 44.38; H, 3.60; N, 9.09. Calcd for C$_{92}$H$_{80}$F$_{24}$N$_{16}$-P$_4$Pd$_4$·4H$_2$O (%): C, 44.42; H, 3.57; N, 9.01. The single crystals suitable for X-ray determination were grown by the vapor diffusion of diethyl ether into a 1.0 mM solution of **3·4PF$_6$$^-$** in acetonitrile at room temperature.

{[(phen)Pd]$_4$L$^3_2$}(NO$_3$)$_4$ (4·4NO$_3$$^-$). The same procedure as employed for **9·8NO$_3$$^-$** was followed except that H$_2$L^3 (17.2 mg, 0.05 mmol) was used as the starting material. Yield: 55 mg (95%). The PF$_6$$^-$ salt of **4** was obtained as yellow microcrystals

in quantitative yield. ^{1}H NMR (400 MHz, CD$_3$CN, 25 °C, ppm) δ = 8.96−8.94 (d, J = 6.48 Hz, 8H, phen-H$_{2,9}$), 8.56−8.54 (d, J = 6.48 Hz, 8H, phen-H$_{4,7}$), 8.19 (s, 8H, phen-H$_{5,6}$), 7.94−7.91 (dd, J = 6.48 Hz, 8H, phen-H$_{3,8}$), 4.15 (s, 8H, L^4-CH$_2$), 2.40 (s, 24H, L^4-CH$_3$); ESI-MS (acetonitrile) m/z: 1062.0 [**4**·2PF$_6^-$]$^{2+}$, 657.8 [**4**·PF$_6^-$]$^{3+}$, 457.1 [**4**]$^{4+}$. Found: C, 45.20; H, 3.23; N, 9.09. Calcd for C$_{92}$H$_{76}$F$_{24}$N$_{16}$P$_4$Pd$_4$·2H$_2$O (%): C, 45.15; H, 3.29; N, 9.16.

{[(**bpy**)**Pd**]$_4$**L$^3_2$**}(**NO$_3$**)$_4$ (**5·4NO$_3^-$**). The same procedure as employed for **9**·8NO$_3^-$ was followed except that [(bpy)$_2$Pd$_2$-(NO$_3$)$_2$](NO$_3$)$_2$ (39 mg, 0.1 mmol) and **H$_2$L^3** (17.2 mg, 0.05 mmol) were used as the starting material. Yield: 54 mg (95%). The PF$_6^-$ salt of **5** was obtained as yellow microcrystals in quantitative yield. ^{1}H NMR (400 MHz, DMSO-d_6, 25 °C, ppm) δ = 8.68−8.66 (d, J = 8.22 Hz, 8H, bpy-H$_{6,6'}$), 8.52−8.42 (m, 16H, bpy-H$_{3,3'}$; bpy-H$_{4,4'}$), 7.86−7.82 (m, 8H, bpy-H$_{5,5'}$; L^4), 7.33−7.25 (m, 4H), 7.22 (s, 4H), 4.18 (s, 8H, L^4-CH$_2$), 2.43 (s, 24H, L^4-CH$_3$); ESI-MS (acetonitrile) m/z: 1013.6 [**5**·2PF$_6^-$]$^{2+}$, 626.4 [**5**·PF$_6^-$]$^{3+}$, 433.3 [**5**]$^{4+}$. Found: C, 41.91; H, 3.63; N, 9.39. Calcd for C$_{84}$H$_{76}$F$_{24}$N$_{16}$P$_4$Pd$_4$·5H$_2$O (%): C, 41.95; H, 3.60; N, 9.32.

{[(**bpy**)**Pd**]$_4$**L$^4_2$**}(**NO$_3$**)$_4$ (**6·4NO$_3^-$**). The same procedure as employed for **9**·8NO$_3^-$ was followed except that [(bpy)$_2$Pd$_2$-(NO$_3$)$_2$](NO$_3$)$_2$ (39 mg, 0.1 mmol) and **H$_2$L^4** (20.18 mg, 0.05 mmol) were used as the starting material. Yield: 63.6 mg (95%). The PF$_6^-$ salt of **6** was obtained as yellow microcrystals in quantitative yield. ESI-MS (acetonitrile) m/z: 1004.4 [**6**·2PF$_6^-$]$^{2+}$, 621.5 [**6**·PF$_6^-$]$^{3+}$, 429.8 [**6**]$^{4+}$. Found: C, 50.73; H, 3.89; N, 7.82. Calcd for C$_{122}$H$_{100}$-F$_{24}$N$_{16}$P$_4$Pd$_4$·5H$_2$O (%): C, 50.78; H, 3.84; N, 7.77.

{[(**bpy**)**Pd**]$_4$**L$^5_2$**}(**NO$_3$**)$_4$ (**7·4NO$_3^-$**). The same procedure as employed for **9**·8NO$_3^-$ was followed except that [(bpy)$_2$Pd$_2$-(NO$_3$)$_2$](NO$_3$)$_2$ (39 mg, 0.1 mmol) and **H$_2$L^5** (35.05 mg, 0.05 mmol) were used as the starting material. Yield: 50 mg (75%). The PF$_6^-$ salt of **7** was obtained by adding a 10-fold excess of KPF$_6$ to its aqueous solution at 60 °C, which resulted in the

immediate deposition of **7**·4PF$_6^-$ as yellow microcrystals in quantitative yield. ^{1}H NMR (500 MHz, CD$_3$CN, 25 °C, ppm) δ = 8.36−8.24 (m, 16H, bpy-H$_{6,6'}$; bpy-H$_{3,3'}$), 8.10−8..01 (m, 8H,; bpy-H$_{5,5'}$), 7.70−7.63 (m, 8H, bpy-H$_{4,4'}$), 7.00 (s, 2H; L^5-Ph-H), 3.83 (s, 8H; L^5-CH$_2$), 2.27 (s, 6H), 2.12 (s, 9H), 2.06 (s, 24H); ESI-MS (acetonitrile) m/z: 1255.1 [**7**·4PF$_6^-$]$^{2+}$, 788.1 [**7**·3PF$_6^-$]$^{3+}$. Found: C, 38.88; H, 4.46; N, 8.86. Calcd for C$_{82}$-H$_{84}$N$_{16}$F$_{24}$P$_4$Pd$_4$·13H$_2$O (%): C, 38.88; H, 4.38; N, 8.85. The single crystals suitable for X-ray determination were grown by the vapor diffusion of diethyl ether into a 1.0 mM solution of **7**·4PF$_6^-$ in acetonitrile at room temperature.

{[(**bpy**)**Pd**]$_4$**L$^6_2$**}(**NO$_3$**)$_4$ (**8·4NO$_3^-$**). The same procedure as employed for **9**·8NO$_3^-$ was followed except that [(bpy)$_2$Pd$_2$-(NO$_3$)$_2$](NO$_3$)$_2$ (39 mg, 0.1 mmol) and **H$_2$L^6** (27.1 mg, 0.05 mmol) were used as the starting material. Yield: 53 mg (95%). The PF$_6^-$ salt of **8** was obtained as yellow microcrystals in quantitative yield. ^{1}H NMR (400 MHz, CD$_3$CN, 25 °C, ppm) δ = 8.08−8.06 (m, 16 H, DBM-PhH), 7.78 (d, J = 5.6 Hz, 8 H, bpy-H$_{6,6'}$), 7.31−7.35 (m, 24 H, bpy-H$_{3,3'\ 4,4'\ 5,5'}$), 7.15−7.11 (m, 8H, DBM-PhH), 6.97−6.93 (m, 16H, DBM-PhH), 6.28 (s, 8H, PhH), 3.86 (s, 8H, CH$_2$); ESI-MS (acetonitrile) m/z: 759.1 [**8**·PF$_6^-$]$^{3+}$, 532.6 [**8**]$^{4+}$. Found: C, 50.65; H, 3.40; N, 8.08; Calcd for C$_{116}$H$_{88}$N$_{16}$ F$_{24}$ P$_4$Pd$_4$·2H$_2$O (%): C, 50.71; H, 3.37; N, 8.16.

Supporting Information Available: ^{1}H NMR and ^{13}C NMR-spectra of **a**−**f** and **H$_2$L^n** (n labeled by 1, 2, 3, 4, 5, 6). Tables of selected bond lengths and angles for **1**, **3**, and **7**; Packing diagrams of **1**, **3**, and **7**; X-ray crystallographic files in CIF format for complexes **1**, **3**, and **7**; and UV−vis and fluorescence spectra. This material is available free of charge via the Internet at http://pubs.acs.org.